Multimedia Tools and Applications (2024) 83:40039–40055
https://doi.org/10.1007/s11042-023-17109-8

Effective recognition of glaucoma using SIFT and RFSO classifier

S. Sheeba Jeya Sophia[1] · **S. Diwakaran**[1]

Received: 18 May 2023 / Revised: 12 September 2023 / Accepted: 18 September 2023 /
Published online: 7 October 2023

Abstract
One of the most serious eye illnesses, glaucoma affects the astrocytes and optic nerve fibres, causing irreversible damage to the eyes. As a result, glaucoma early identification is crucial in the medical industry. Retinal image-based detection falls within the category of non-invasive ways of detection among the many techniques. Automatic periodical screening can aid in the prompt detection of retinal glaucoma, while also easing the workload of skilled ophthalmologists. Effective glaucoma treatment can also lessen the severity of vision impairments brought on by the disease's advanced stages. The retinal fundus dataset is used in this paper to undertake a novel glaucoma detection procedure. Additionally, the Scale-invariant feature transform (SIFT) is a widely used method for feature extraction and clustering in picture classification tasks. The characteristic is robust to variations in illumination, noise, partial occlusion, and minor changes in viewpoint in the photos. It is independent of the scale and orientation of the images. The real-time glaucoma screening system is suggested for use with this clustering approach. Convolutional neural network (CNN) classifier optimization is performed using a mix of the SIFT and Rooster Food Search optimization (RFSO) based algorithms for exploration and exploitation procedures. To assess whether a retina is glaucomatous or healthy, the resulting optic disc area is used. As a result, the study was presented based on efficient clustering, precise classification, and the use of various data sets, including the LAG and Rim-One database. The suggested technique was created in MATLAB and tested on this database. The suggested strategy produced accuracy levels above 95% and performed better on comparisons for additional metrics like clustering and classifier-related factors. In order to help researchers conduct additional study on glaucoma detection, we provide research difficulties and their respective solutions.

Keywords Glaucoma · Retinal images · SIFT clustering & feature extractions · RFSO classification

✉ S. Sheeba Jeya Sophia
s.sheebajeyasophia@klu.ac.in

[1] Department of Electronics and Communication Engineering, Kalasalingam Academy of Research and Education, Krishnankoil, India

1 Introduction

Glaucoma is the most common factor in permanent blindness across the globe and is linked to a lower quality of life [1] and is linked to a lower quality of life. It currently affects about 70 million people worldwide, would likely affect 111.8 million people by the year 2040 [2]. Elevated intraocular pressure is presently the only modifiable risk factor for this illness. In general, glaucoma affects older people more frequently, especially those with severe diabetes, nearsightedness, or high BP (blood pressure). The optic nerve is the nerve fibre that carries visual data from the eye to the brain, is gradually damaged by glaucoma. Glaucoma rarely affects eyesight in its early stages, so patients typically aren't aware of it. Peripheral vision loss brought on by glaucoma's latter stages might lead to irreversible blindness. But a timely diagnosis and appropriate care can slow the disease's course and prevent eyesight loss.

As a result, early detection of this irreversible glaucoma condition is significant [3]. Many different forms of glaucoma can exist [4]. Additionally, vital components including ophthalmoscopy, tonometry, gonioscopy, perimetry, and pachymetry should be examined before making a glaucoma diagnosis. The diagnosis of glaucoma is then made using the patient's intraocular pressure (IOP), tests for visual field loss, and an ophthalmoscopy examination of the optic nerve head (ONH) [5]. Digital fundus cameras, optical coherence tomography (OCT), IOP measurements, ONH evaluations, retinal nerve fibre layer (RNFL), and visual field defects can all be used to test for glaucoma [4].

IOP increases quickly as a result of the eyes' drainage system malfunctioning. The fluid pressure in the eyes then continues to rise, damaging the eyes' optic nerve [6] and impairing vision permanently [7], which results in the irreversible condition known as glaucoma. Additionally, one of the primary causes of glaucoma disease is the decreased thickness of the RNFL as a result of the damaged RNFL [8]. Additionally, a number of factors, including the ONH, the nerve fibre layer, structural alterations, and the functional stoppage, might cause glaucoma problem in the visual field simultaneously [9].

Thus, regular eye exams for potential glaucoma sufferers are necessary to aid in the disease's early diagnosis. An ophthalmologist will manually evaluate a patient's retinal picture during an eye exam to check for the presence of glaucoma symptoms. It can take a long time to manually analyse retinal pictures [10]. To ensure the accuracy of the performed diagnosis, the images should also be examined by highly qualified ophthalmologists [11].

One of the most crucial noninvasive methods in medicine [12] for identifying glaucoma also allows ophthalmologists to differentiate between healthy and unhealthy retinas [13]. The main benefit of retinal fundus pictures is that they are generally simple to obtain in clinical settings. Then, to identify glaucoma-related eye illnesses, data from digital image analysis is extrapolated [14].

In this study, a suggested Rooster Food Search optimization (RFSO) based CNN is used to detect glaucoma. Using the features of varied the hierarchy of chicks and search directions; the proposed RFSO-based CNN focuses heavily on detecting the target item. The input image is initially taken from the dataset and segmented using SIFT module. The feature extraction module extracts the features from the segmented result, which helps to improve detection accuracy. Based on the bias and weights attached to the neurons, the CNN classifier detects the target item in the best possible way, with the weights calibrated are tuned optimally by the newly developed RFSO algorithm [15, 16]. The proposed RFSO method is used to carry out the CNN training process, which then changes the weights using a modified SIFT algorithm equation. Thus, employing various clustering and

classification progress ideas, this sickness can be detected effectively. Briefly stated, the paper's contribution is as follows:

- In this research, the application of SIFT-based clustering in CNN models of neural networks is reviewed in order to increase performance.
- It takes into account a number of evolutionary algorithms from the RFSO viewpoint.
- The paper makes recommendations for tightening the connections between SIFT, RFSO, and deep learning.
- Comparing the newly proposed approach to previous pertinent techniques, the simulative analysis tends to show that it can produce better results.

2 Related reviews

In our ageing culture, glaucoma is the main cause of permanent blindness [2]. Chronic neuropathy damages structurally the optic nerve fibres, causing external and internal alterations to the optic disc that ultimately cause functional vision loss. The optic nerve head (ONH), also known as the optic disc, has certain alterations that are linked to glaucoma [17]. Ophthalmologists assess the ONH during optic disc photo analysis and clinical examination, looking for characteristic alterations including generalised or focal neural rim thinning.

In the field of medical image processing, convolutional neural networks (CNN) and deep learning models in particular are setting new standards. These models are being used in numerous healthcare applications, such as the diagnosis of pneumonia on chest CT and the dermatologist-level classification of skin cancer [18, 19]. The main area of study in ophthalmology has been the ability of CNNs to diagnose serious eye conditions like diabetic retinopathy [20], age-related macular degeneration [21], and cataract [22] using readily available to a lesser extent, colour fundus photos and, optical coherence tomography (OCT) scans.

Deep learning-based diagnostic models may help overcome the problem of glaucoma underdiagnosis while limiting the false positive rate [23]. In the area of automated glaucoma diagnosis [24] and glaucoma-related parameters [25] from fundus pictures employing CNNs, successes have previously been recorded. Due to the fact that picture characteristics are no longer manually created and chosen, those outcomes came at the expense of less information about the predictive model's decision-making process. Transparency in decision-making, also known as CNN explainability, is essential to fostering trust in the potential application of deep learning to medical diagnosis.

However, due to the random selection of hyper-parameters, CNNs may perform less effectively and be unable to distinguish between glaucoma severity levels. The value of the hyper-parameter regulates convergence speed and directs the approach to the ideal minimum or maximum [26]. Out of all typical approaches, the optimization process provides a better level of parameter selection accuracy, but it may result in a high level of computing complexity. Numerous algorithms for swarm-based optimization have been studied. This deep learning classifier is incorporated into the system. Additionally, the same CNN approach is used, but SIFTS feature clustering incorporates the variances, and the RFSO based optimizers are chosen for the effective outcomes.

It is suggested to use the Chicken Swarm Optimization (CSO) method, a newly created bio-inspired optimization technique. It imitates the hierarchical configuration of the

chicken swarm and its behaviour. One rooster and numerous hens and chicks make up each of the different groupings that make up the chicken swarm. Various types of chickens adhere to various laws of motion. Different chickens compete against one another in a set hierarchical sequence. This process is modified as rooster food search algorithm in our approach.

3 Methodology

The chickens and their eggs are largely kept as a source of food because they are one of the most often kept domestic animals. Domestic chickens are social creatures that coexist in flocks [27]. Even after several months apart, they remain cognitively advanced and can recognise more than 100 people. They communicate using more than 30 different sounds, including clucks, cackles, chirps, and cries. These sounds contain a wealth of information about nesting, food discoveries, mating, and danger.

The chickens would gain knowledge for making judgments not only via trial and error but also through their prior knowledge and that of others. In the social interactions of chickens, hierarchical order is important. In a flock, the dominant chickens will rule over the losers. Together with the more obedient hens and roosters that are near the edge of the group, there are the more leading hens that stick close to the head roosters. The social structure would be temporarily upset by adding or removing hens from a group until a clear hierarchy was formed.

When they locate food, the roosters might request their fellow group members to eat first, but the dominant individuals have first access to it. When chickens rear their young, they exhibit the same kind of graciousness. Yet, people from various groups do not share this characteristic. As other chickens from a different flock enter their region, roosters make a loud call.

The behaviour of the chicken varies generally according to gender. The group's dominant rooster actively seeks out food and engages in conflict with intruding chickens. When foraging for food, the dominant chickens would almost always follow the head roosters. But when it came time to look for food, the submissives would reluctantly stand outside the group. Different chickens compete against one another. The chicks explore the area around their mother in quest of nourishment.

The chickens can't work together because they are all too simple. When viewed as a swarm, however, they might cooperate as a group to look for food while following a set hierarchy. We are motivated to create a novel algorithm by the swarm intelligence that can be connected to the situation at hand that needs to be optimized [27–29].

The application for the target illness detection is a key field in the medical research community due to the increased attention glaucoma has received in recent years. Developing a strategy to precisely recognise the target object, however, presents a difficult problem with glaucoma. In order to accomplish the glaucoma detection, a successful method called RFSO-based CNN classifier is suggested in this research. The segmentation module receives input from the LAG and Rim-One datasets, which is then used to divide the image into several segments using SIFT [16].

The feature extraction module extracts the statistical and texture features from the segmented output before it is sent on to the segmentation step. The localization Sub-net and SIFT statistical characteristics are used to extract the texture features. The CNN classifier accurately detects glaucoma in retinal images using the retrieved features. Additionally, the

suggested RFSO technique, which combines SIFT [15] with chicken swarm optimization (CSO) [28], is used to train the CNN. Sending the image and the target item to the CNN classifier as a query allows for the detection of the target object. The CNN recognises the matched result more precisely by comparing the query object to the HSI object. The proposed SIFT-based CNN's schematic diagram for target glaucoma detection utilising trained datasets is shown in Fig. 1.

4 Proposed concept

The submitted work is explained individually in this section. They are SIFT model, RFSO, CNN as well as their optimization scheme to enhance their detection progress.

4.1 SIFT algorithm for image feature detection

Even though some forms of glaucoma are related with the retinal vessels and typically have abnormal size and shape, it is still challenging to automatically identify all of them. We suggest a fresh approach in this strategy to address these issues. In order to address the detection of both isolated and vessel-connected retinal abnormalities, a new technique is introduced. The SIFT method uses the Gaussian difference of images to identify extreme spots, but this method clusters feature points, making it difficult to match them later. The number of SIFT feature points found in many flat locations remained low, despite the fact that in some flat areas, SIFT could find feature spots.

Because the technique relies on finding intersections and corners present in the thermal map; the characteristics that are found mostly surround flat and curved patterns. As a result, there are few feature points found in these places. As a result of the absence of paired control points existing in these locations, the picture registration performance would otherwise

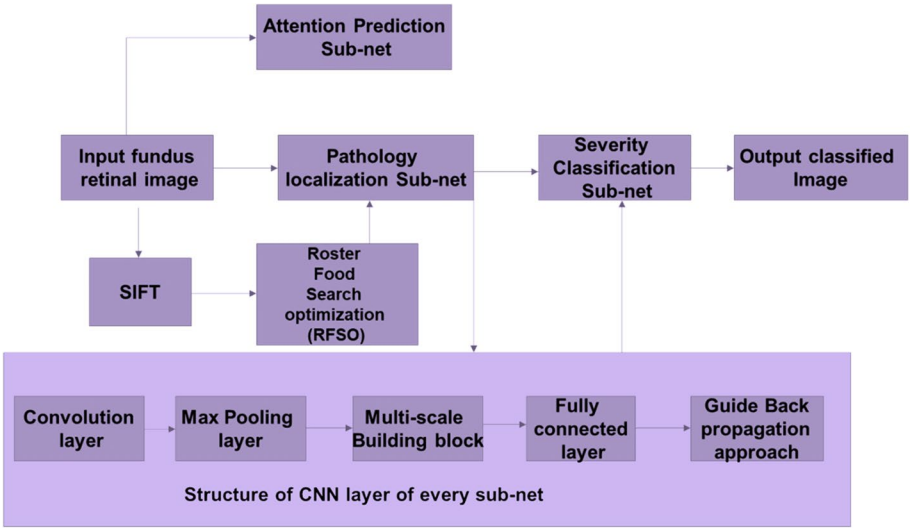

Fig. 1 The conceptual design of the proposed SIFT-based CNN

be subpar. In disparity, the projected concept recognised features in those flat sections and improved the performance. The three feature point detection requirements were all satisfied by the suggested method. In particular, the suggested method produced good feature point detection results even for the medical images, which contained several flat regions.

The picture gradients serve as the foundation for SIFT, which is invariant to scaling and rotation [25]. Because it is rotation-invariant, we can still get the same result even if we rotate the image. Since it is scale invariant, changing the image scale has no impact on the outcome. This technique also exhibits strong resilience to more sophisticated transformation and lighting alterations. SIFT utilises the adaptive Gaussian (AG) distribution function to extract significant points and feature vectors. This adaptive function is modified in place of general Gaussian distribution function. This is used to adapt with respect to the trained set in order to extract the similar features.

For training and testing the datasets in SIFT, the most predictable features are extracted and grouped together. We will employ convolutional neural networks to learn contextual dependencies while maintaining spatial neighbourhood dependences, which are crucial for processing of image input data.

4.2 RFSO model

The CNN classifier is trained using the suggested CS algorithm to update the weights in the best possible way depending on the best fitness metric. The swarming behaviour of chickens and the hierarchical arrangement of chicks are combined in the bio-inspired optimization algorithm known as CSO. To handle the unbalanced data, SSD is used successfully. The suggested CS algorithm uses the parametric information from both algorithms to improve detection performance, making it highly targeted at identifying the target object from an image.

The CNN classifier is trained to optimally upgrade the weights depending on the best fitness metric using the suggested RFSO technique. The bio-inspired optimization technique known as RFSO combines the swarming behaviour of chickens with the hierarchical order of chicks. SIFT is a useful tool for handling the unbalanced data. The suggested RFSO approach incorporates the parametric information from both algorithms to improve identification performance, making it well suited for discovering the goal using glaucoma images. The chicken swarm group in RFSO is divided into a number of subgroups, including chicks, roosters, and hens. There is some competition between the chicken groups in this situation because the chickens experience various laws of motion. The optimization approach is able to attain exceptional performance in glaucoma detection thanks to the stochastic exploration of SIFT and the swarming activities of RFSO.

i. Solution encoding: The ideal solution is chosen depending on the weight and the fitness measure using a representation of a solution vector.
ii. Fitness function: To determine the best option, the fitness function is assessed. Here, the optimum method for locating the target objects is determined to be the chicken with the highest fitness value. The chickens classified as having the lowest fitness value are labelled as chicks, while the other chickens are handled as hens. Based on the fitness value, the fitness function is calculated to find the target item.
iii. Variation in the rooster location: The right to access food among the swarm cluster belongs to the rooster. The roosters steer clear of other swarms so that they can consume the food, while the chickens follow their way to find it. Furthermore, among the

group, virtual chickens steal food from other swarms. Instead of the worst rooster, the best rooster searches for food over a larger area.

iv. Chick position: To find the food, the hen follows the rooster's course. It plunders the food of other swarm members. As a result, dominating females benefit more than submissive females.

v. Assessing the viability: The fitness metric is evaluated to determine the best option. However, it is determined that the fitness rate by means of the lowest error value is the best option. The fitness level is assessed here.

vi. Termination: The aforementioned processes are continued until the maximum iterations have been reached or the best solution has been found.

4.3 CNN model

According to Fig. 1, the basic architecture of the suggested CNN has been developed using bio-inspired optimization technique. The ROI sub-group prediction, Defect area sub-group segmentation, and severity sub-group classification are the three sub-groups that make up the CNN structure. Fundus RGB channels are used as the CNN structure's input and its outputs are segmented defect area and severity graded glaucoma level using SIFT feature descriptors. Because the study's findings indicate that the ROI is concentrated in tiny locations and on multiple scales, the first CNN sub-group is studying the ROI unit to anticipate human responsiveness in glaucoma diagnosis. The second segmenting group receives the projected ROI region and uses the feature it has extracted to identify the faulty area. While segmenting sub-group and the normal area, the projected region is helpful. The last subgroup uses the feature of this sub-clutch in addition to the projected ROI map to output both negative and positive glaucoma. If it is positive, the level of glaucoma will be output. CNN's organisational model is built on residual networks. In order to increase the non-linearity of CNN and speed up convergence, a normalisation layer and a ReLU layer are added after each convolutional layer. Three subgroups are used to account for losses throughout the end-to-end supervision of the CNN structure training.

The three local sub-net CNN structure is implemented using the following steps.

- The three sub-nets include one for predicting attention, one for locating diseased areas, and one for classifying glaucoma.
- The initial part detects the defected part using the extracted attention maps and features from the first sub-net, which produces the attention map and predicts the area of glaucoma.
- In the next CNN sub-net, SIFT and Rooster Food Search optimization (RFSO) is proposed to cluster, feature extract and to tune the learning rate of the BP-Back propagation approach and activation function.
- The final sub-net divides the input image into glaucoma cases of varying severity and glaucoma-negative cases.

Figure 2 shows ROI, kernels and convolutional diagram along with the flow of feature detector SIFT and RFSO for estimating the optimal solution. The attention plans of fundus images are created by the ROI prediction sub-group. Then, glaucoma detection and defect area localization are accomplished using these attention maps. The input fundus photos are $224 \times 224 \times 3$ in size. It is served to the 7×7 kernel convolutional layer and then to the single max-pooling layer. The features then shift into eight building pieces in order to extract

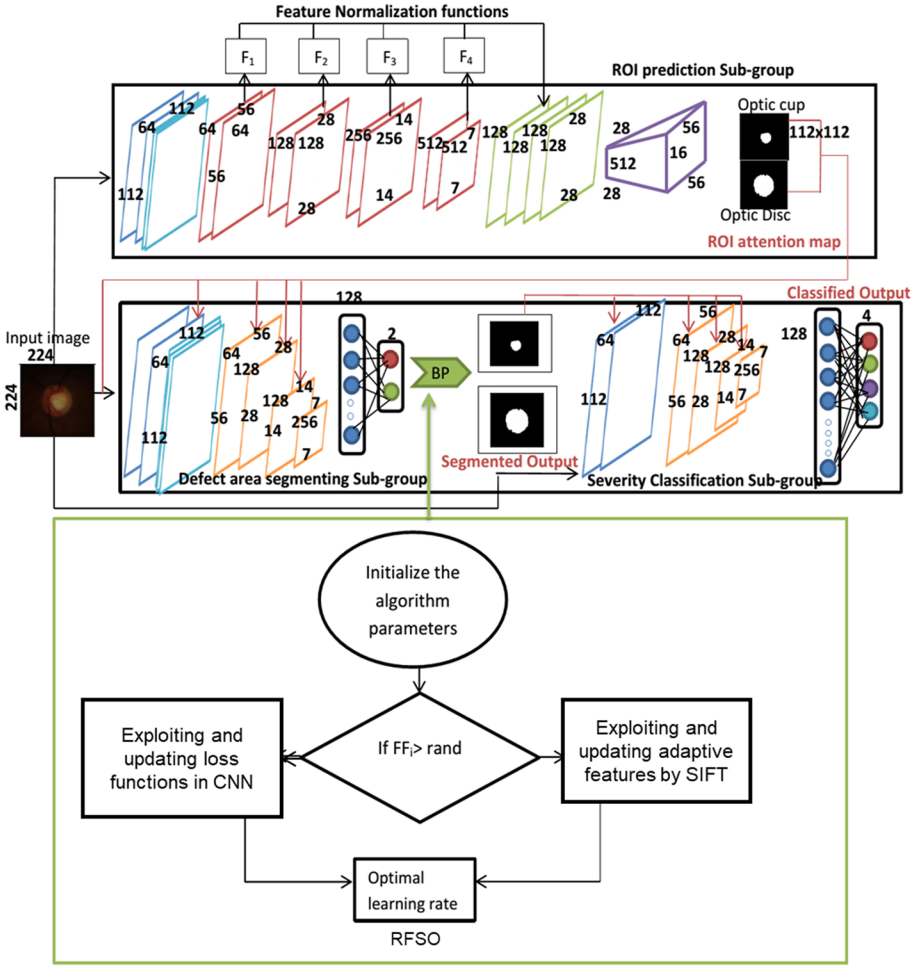

Fig. 2 The schematic flow of CNN with RFSO-SIFT

hierarchical characteristics. Following this, feature normalization is used to process the features of the four hierarchical building blocks to produce the four $28 \times 28 \times 128$ features. A $28 \times 28 \times 512$ deep multi-scale feature is created by concatenating the features.

The de-convolutional layer receives these features after which it creates attention maps of size $112 \times 112 \times 1$, with values ranging from 0 to 1. It contains layers of 4 convolutional and 2 de-convolutional. The purpose of these attention maps is to make it simple for subgroups of segmentation and classification parts to focus on the ROI region.

Convolutional layers and completely connected layers make up this subgroup. The recovered feature maps from the input fundus image are utilised to mask the defect area at various layers using the ROI attention maps. Hence, using the input RGB channel fundus pictures as input I, the fully connected layer f_{out} generates the visualisation map of the defect area using guided back propagation (BP). This function includes and accepts input from the ReLU activation function. This sub-group is made up of 4 multi-scale building blocks, 1 max-pooling layer, and 7×7 convolutional layers. To extract multi-scale features,

this multi-scale building block comprises 5 layers of convolutional channels with various kernel sizes. The categorization results are finally generated using 2 completely connected layers. The hyper-parameters from SIFT features and the CNN classification are optimized using RFSO algorithm.

4.4 Optimization of SIFT operator

Certainly, assume that the input image $\bar{I}(x,y)$ has a scale space $\hat{S}(x,y,\sigma)$, which can be written to that corresponding input as,

$$\hat{S}(x,y,\sigma) = \hat{G}(x,y,\sigma) * \bar{I}(x,y) \tag{1}$$

In which * denotes the convolution process and is a variable-scale Gaussian function that has been modified and defined as a new, rewriteable adaptive Gaussian function as

$$\hat{G}(x,\ y,\sigma) = \frac{1}{\sigma\sqrt{2\pi}} e^{\frac{-1}{2}\left(\frac{x-y}{\sigma}\right)^2} \tag{2}$$

The scale coordinate is (x,y), and the smoothness of the input image is (σ). A method called Difference of Gaussian Scale-Space (DOG) is developed to find the stable keypoint in scale space. By convolution of a Gaussian difference with the image $\bar{I}(x,y)$, DOG discovers local maxima and minima of $Đ(x,y,\sigma)$. This procedure is writeable as

$$\begin{aligned} Đ(x,y,\sigma) &= (\hat{G}(x,y,ķ\sigma) - \hat{G}(x,y,\sigma)) * \bar{I}(x,y) \\ &= \hat{S}(x,y,ķ\sigma) - \hat{S}(x,y,\sigma) \end{aligned} \tag{3}$$

The aforementioned process searches across all scales and image locations to find probable keypoints that are independent of scale and orientation. As a result, a group of keypoint candidates can be found. The essential points will then be precisely localised. Keypoints with low contrast or those that are awkwardly localised along an edge will be eliminated in this step.

The assignment of orientation to each keypoint is the third step in the SIFT algorithm. These gradient orientations within an area of sample points to produce an orientation histogram surrounding the keypoint is used to carry out this function. The 360 degrees of orientations are represented by the histogram's 36 bins. The histogram angle positioning can be utilized to precisely establish the keypoint orientation since the peak of the histogram represents the dominant direct of the neighbourhood gradient of the keypoint. The keypoint descriptor is the final phase of the SIFT method. A K-by-4 matrix can be created from the procedures previously mentioned, and the four values for a keypoint position are present in each row of the matrix. (column, row, orientation, scale). A K-by-128 matrix with an invariant descriptor for each of the K keypoints in each row and a 128 vector values normalised per unit length is the result of the SIFT feature.

In particular, the closest neighbour method is used to identify the most suitable candidates for each feature point. The key point for an invariant descriptor with the smallest Euclidean distance vector is defined here as the nearest neighbour. Establishing a ratio between the closest neighbor's distance and the length to the next-closest neighbour is a useful metric for matching validation. The RFSO technique, which is utilised to offer the improved adaptive

SIFT feature detectors for both the ground truth and the test (or input) image, is employed to optimise this k value.

4.5 Optimization using RFSO concept

Suppose that the letters *HN, RN, MN*, and *CN*, respectively, stand for the number of hens, roosters, mother hens, and chick hens. The most desirable RN chickens would be considered roosters, whereas the least desirable CN chickens would be thought of as chicks. The remainder is handled like hens. All N virtual chickens look for food in a D-dimensional space as represented by their positions, $x_{i,j}^{st}(\mathrm{i} \in [1, \ldots, \mathrm{N}]), \mathrm{j} \in [1, \ldots, \mathrm{D}])$ at step time (*st*). The simplest optimization problems are used in this approach. Hence, the chickens with the highest RN minimal fitness values are the best *RN* chickens. The overall procedure is to be followed in RFSO for determining the best fitness rate as per the upcoming steps.

Pseudo code for RFSO algorithm

i. **For** $i = 1 : N$
  a. If i == rooster, then Fill its location/solution by eq. (1); End if
  b. If i == hen, then Fill its location/solution by eq. (3); End if
  c. If i == chick, then Fill its location/solution by eq. (6); End if
  d. Estimate the new/fresh solution;
  e. If this solution is healthier than its previous one, update it;
ii. End for

For ease of simulation, assume that the roosters with better fitness values are able to look for food in a larger variety of locations than the roosters with lower fitness values can. This can be expressed as follows.

$$x_{i,j}^{st+1} = x_{i,j}^{st} * (1 + randn(0, \sigma^2)) \tag{4}$$

$$\sigma^2 = \begin{cases} 1, & if\ f_i \le f_k \\ \exp\left(\frac{f_k - f_i}{|f_i| + \varepsilon}\right), & otherwise\ k \in [1, \mathrm{N}], \mathrm{i} \ne \mathrm{k} \end{cases} \tag{5}$$

This σ value is produced as an adaptive Gaussian function from Eq. (2). The Gaussian distribution *Randn* $(0, \sigma^2)$ affords zero mean and a standard deviation (σ^2). The tiniest constant in a computer is ε, used to prevent zero-division errors. The index of a rooster, k, is randomly selected from the group of roosters, and f is the matching x's fitness value. The hens could go for a food hunt with the roosters in their group. Also, despite being restrained by the additional chickens, they should haphazardly steal the tasty food that other birds had discovered. The extra dominant hens should have an advantage over the additional submissive ones in the food competition. These phenomena can be formally expressed as follows.

$$x_{i,j}^{t+1} = x_{i,j}^{t} + S1 * Rand * (x_{r1,j}^{t} - x_{i,j}^{t}) + S2 * Rand * (x_{r2,j}^{t} - x_{i,j}^{t}) \tag{6}$$

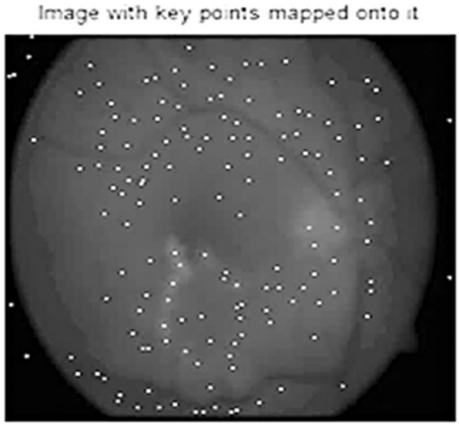

Fig. 3 SIFT image with key-point detections

$$S_1 = exp(f_i - f_{r1})/(abs(f_i + \varepsilon)) \tag{7}$$

$$S_2 = exp(f_{r2} - f_i) \tag{8}$$

In which, *Rand* is a constant random number among [0, 1]. In this case. Although $r2 \in [1, \ldots, N]$ is a chicken index (either hen or rooster) rooster, $r1 \in [1, \ldots, N]$ is a rooster index, who is the i^{th} hen group-mate. It is randomly selected from the swarm $r1 \neq r2$.

Observably $(f_i > f_{r1})$ and $(f_i > f_{r2})$, as a result $S2 < 1 < S1$. The i^{th} hen would first go for food-foraging, then the other chickens, assuming $S1 = 0$. Larger the gap between the two placements of chicks, the lower will be S2 and greater the fitness value differential between them. Hence, the hens would be less likely to steal the food that other chickens had found. Because there are competitions within a group, S1's formula form is different from S2's. For ease of use, the competitions amongst chickens in a group are simulated as the fitness values of the chickens in relation to the fitness value of the rooster. If $S2 = 0$, the i^{th} hen would look for food within its own domain. The rooster has a special fitness value for that

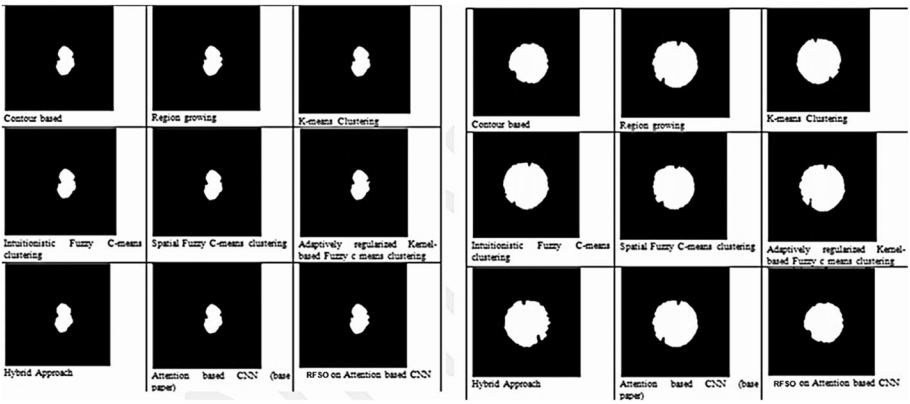

Fig. 4 Segmentation comparisons of several approaches

Table 1 Performance comparisons of proposed approach

Segmentation Approaches	Data set	Metrics							
		TP	FP	TN	FN	ACC	SD	DS	JD
Super pixel classification	LAG	0.76	0.15	0.84	0.23	88.0	0.20	0.84	0.20
	Rim-one	0.77	0	1.00	0.22	88.9	0.28	0.85	0.19
Contour based	LAG	0.78	0.14	0.85	0.21	88.8	0.20	0.85	0.19
	Rim-one	0.78	0	1.00	0.21	89.5	0.26	0.86	0.18
Region growing	LAG	0.78	0.13	0.86	0.21	89.2	0.20	0.86	0.18
	Rim-one	0.79	0	1.00	0.20	89.9	0.21	0.87	0.17
K-means Clustering	LAG	0.79	0.13	0.86	0.20	89.6	0.18	0.86	0.19
	Rim-one	0.80	0	1.00	0.19	90.0	0.19	0.87	0.17
Intuitionistic Fuzzy C-means clustering	LAG	0.80	0.12	0.87	0.19	90.3	0.17	0.88	0.16
	Rim-one	0.82	0	1.00	0.17	91.1	0.17	0.89	0.14
Spatial Fuzzy C-means clustering	LAG	0.81	0.11	0.88	0.18	90.7	0.18	0.89	0.15
	Rim-one	0.82	0	1.00	0.17	91.3	0.18	0.90	0.14
Adaptively regularized Kernel-based Fuzzy c means clustering	LAG	0.82	0.10	0.89	0.17	91.4	0.17	0.89	0.14
	Rim-one	0.84	0	1.00	0.15	92.4	0.17	0.90	0.13
Attention based CNN (base paper)	LAG	0.83	0.09	0.90	0.15	91.8	0.11	0.91	0.10
	Rim-one	0.85	0	1.00	0.12	93.0	0.15	0.92	0.09
RFSO-SIFT based CNN	LAG	0.92	0.02	0.90	0.20	95.18	0.08	0.97	0.9
	Rim-one	0.94	0.01	0.90	0.15	94.24	0.04	0.95	0.7

group. Hence, the closer S1 approximates to 1 and the smaller the distance among i^{th} hen's position and that of its groupmate rooster, the lower the i^{th} hen's fitness value is. So, the more dominant hens would be more likely to devour the food than the more submissive chickens. To find nourishment, the chicks move about their mother. Here is how it is put together as per the formula,

$$x_{i,j}^{t+1} = x_{i,j}^{t} + FL * (x_{m,j}^{t} - x_{i,j}^{t}) \tag{9}$$

where $x_{m,j}^{t}$ denotes the mother's location for the i^{th} chick $(m \in [1,\ldots,N])$. The parameter FL ($FL \in (0,2)$) indicates that the chick would follow its mother while foraging for food. Given the variations in each chick, the FL would randomly select a number between 0 and 2. This value is utilized in both the SIFT and CNN classifier for optimizing the specific parameters to attain the better outcome on comparing with the relevant schemes [26].

5 Result analysis

The newly proposed RFSO-based CNN are simulated, analyzed and compared in this section. The experimentation of the proposed model is carried out in the specified MATLAB tool [26]. Glaucoma detection is carried out using the LAG database. There are 4,878 positive and 6,882 negative glaucoma samples among the 11,760 fundus pictures. The Chinese Glaucoma Study Alliance (CGSA) and Beijing Tongren

Table 2 Performance comparisons of proposed approach

Database	Method	Accuracy				Sensitivity				Specificity			
		1	2	3	4	1	2	3	4	1	2	3	4
LAG	Chen et al.	85.4	85.2	88.6	89.2	83.2	85.1	87.12	89.4	80.0	60.2	65.3	89.0
	Li et al.	86.5	89	90	89.7	88.3	89.1	90.25	91.4	67.8	61.3	63.25	88.4
	Li, L et al.	92.1	90	95.34	96.2	91.1	92.5	94.3	95.4	85.2	75.2	78.2	96.7
	Proposed	96.2	95	98.12	97.3	88.2	86.4	92.5	95.4	86.3	81.2	83.2	98
RIM-ONE	Chen et al.	82.3	83.2	75	80.0	60.2	65.3	67.45	69.6	83.2	85.1	87.12	87.0
	Li et al.	86.4	85.1	65	67.8	61.3	63.25	65.4	67.4	88.3	89.1	90.25	68.1
	Li, L et al.	92.63	86.9	72.16	85.2	75.2	78.2	82.6	84.8	91.1	92.5	94.3	85.5
	Proposed	96.66	95.47	92	89.9	88.8	85.9	89.12	89.12	92.12	90.12	94.21	90.12

Table 3 Performance comparisons of several approaches

Database	Method	AUC				F 1 Score			
		1	2	3	4	1	2	3	4
LAG	Chen et al.	0.91	0.92	0.93	0.953	0.84	0.85	0.89	0.886
	Li et al.	0.92	0.95	0.954	0.960	0.85	0.89	0.91	0.954
	Li, L., et al.	0.92	0.95	0.98	0.983	0.88	0.90	0.93	0.954
	Proposed	0.92	0.93	0.95	0.99	0.91	0.95	0.96	0.964
RIM-ONE	Chen et al.	0.75	0.78	0.82	0.831	0.65	0.68	0.69	0.711
	Li et al.	0.65	0.68	0.72	0.731	0.61	0.63	0.65	0.654
	Li, L., et al.	0.81	0.85	0.89	0.916	0.81	0.82	0.825	0.837
	Proposed	0.95	0.93	0.956	0.967	0.89	0.90	0.	0.92

Hospital provided this LAG database. The LAG database is initially graded on a three-tier scale. The selected professional ophthalmologists independently evaluate each image in light of the referable glaucomatous optic neuropathy criteria. As a result, all samples in the LAG database are classified as having glaucoma, either positively or negatively. The initial parameters setting conditions are considered similar to that of the previously developed work [26].

Figure 3 presents the result of feature point detection with key points mapped in the test image using SIFT concept. With the use of the ROI attention maps from the first sub-group, the optic cup and optic disc of the fundus images are separated individually in the second group. The ROI can either be indicated as tiny or large in the attention maps, as shown in Fig. 4, because the results of the data analysis demonstrate that the ROI vary in scale. The size of the attention map determines whether glaucoma is positive or negative.

In Table 1, the newly developed RFSO-based method is assessed and contrasted with eight additional heuristic methods for the detection of glaucoma. Accuracy, specificity, s ensitivity, dice similarity (DS), Standard deviation (SD), and Jaccard Distance (JD) are the metrics that are specifically measured. The proposal has a lower percentage of false positives and false negatives while having a greater rate of true positives and true negatives. Only 0.04% of the optimized CNN varied from the ground truth images, despite having great accuracy. The percentage of similarity and dissimilarity between the output images and the ground truth is determined by dice similarity and Jaccard distance.

Accuracy, sensitivity, specificity, AUC, and F2 Score are the variables that are compared. Along with everything else, performance comparisons are done for classification results with severity distinction, such as negative glaucoma, mild glaucoma, moderate glaucoma, and severe glaucoma as per the Table 2.

The next comparison is made for the parameters such as area under curve (AUC) along with the F1 score values as provided in the Table 3. They are observed for both the databases taken to verify the glaucoma in retinal images.

Thus, the overall simulative analyses are estimated for the segmentation of feature descriptors using SIFT operator and CNN based classification approach are utilized to detect the retinal defects or abnormalities using the well-optimized RFSO scheme.

6 Conclusion

The proposed work effectively segments the blood vessels from the retinal fundus images without manual intervention and provides better segmentation accuracy. The vessel segmentation process with AG filter gives major blood vessels and the more tiny vessels are obtained from the final segmented output. From the segmented image, SIFT features are obtained which gives the precise information about the features of the image and the size is also less. The proposed SIFT and RFSO with CNN based feature selection helps in obtaining better accuracy and reduces computation time. The hyper parameters of CNN classifier are optimized using rooster food search optimization algorithm. It performs effective classification in identifying the retinal abnormalities based on the extracted features. The disease identification accuracy is compared with different methodologies. Also the performance of feature reduction method is observed from the classifier output where the reduced feature set gives better accuracy comparing with the process does not use feature reduction technique. Thus it is also proved that the proposed feature reduction method does not affect the classifier performance as it preserves all the significant information even after the dimension is reduced.

Abbreviations *CNN*: Convolutional neural network; *RFSO*: Rooster Food Search Optimisation; *OCT*: Optical coherence tomography; *SIFT*: Scale-invariant feature transform; *AG*: Adaptive Gaussian

Acknowledgements The authors would like to thank Technical head and team members at Vaigai College of Engineering for their helpful discussions and technical assistance. Also authors would like to thank research scholars of Computer science, Electrical and Electronics, Electronics and Communication Engineering Vaigai College of Engineering for frequency pattern development, which is used in software level checking process.

Authors' contributions Conceptualization, Methodology, Software, Visualization, data duration, Writing-original draft.

Validation, resources, Investigation, Writing-review and editing, supervision, project administration.

Funding No fundings received from any organization.

Data availability My manuscript has no associated data.

Declarations

Competing interests The authors declare that they do not have any conflict of interest with organizations.

References

1. Allison K, Patel D, Alabi O (2020) Epidemiology of glaucoma: the past, present, and predictions for the future. Cureus 12:11
2. Tham YC, Li X, Wong TY, Quigley HA, Aung T, Cheng CY (2014) Global prevalence of glaucoma and projections of glaucoma burden through 2040: a systematic review and meta-analysis. Ophthalmology 121(11):2081–2090
3. Zhang Z, Lee BH, Liu J, Wong DWK, Tan NM, Lim JH, Yin F, Huang W, Li H, Wong TY (2010) Optic disc region of interest localization in fundus image for glaucoma detection in ARGALI. In: Proceedings of International Conference on Industrial Electronics and Applications, Taichung, pp 1686–1689
4. Hussain SA, Holambe AN (2015) Automated detection and classification of glaucoma from eye fundus images: a survey. Comput Sci Inf Technol 6:1217–1224
5. Bock R, Meier J, Nyul LG, Hornegger J, Michelson G (2010) Glaucoma risk index: automated glaucoma detection from color fundus images. Med Image Anal 14:471–481

6. Nayak J, Acharya UR, Bhat PS, Shetty A, Lim TC (2009) Automated diagnosis of glaucoma using digital fundus images. Med Syst 33:337–346
7. Acharya UR, Dua S, Du X, Vinitha Sree S, Chua CK (2011) Automated diagnosis of glaucoma using texture and higher order spectra features. IEEE Trans Inf Technol Biomed 15:449–455
8. Agarwal S, Gulia S, Chaudhary, Dutta MK (2015) A novel approach to detect glaucoma in retinal fundus images using cup-disc and rim-disc ratio. In: Proceedings of International Work Conference on Bioinspired Intelligence, San Sebastian, pp 139–144
9. Mookiah MRK, Acharya UR, Lim CM, Petznick A, Suri JS (2012) Data mining technique for automated diagnosis of glaucoma using higher order spectra and wavelet energy features. Knowl Based Syst 33:73–82
10. Kumar BN, Chauhan RP, Dahiya N (2018) Detection of glaucoma using image processing techniques: a critique. Semin Ophthalmol 33(2):275–228
11. Almazroa A, Burman R, Raahemifar K, Lakshminarayanan V (2015) Optic disc and optic cup segmentation methodologies for glaucoma image detection: a survey. J Ophthalmol 2015:1–28
12. Schacknow PN, Samples JR (2010) Practical, Evidence-Based Approach to Patient Care, the Glaucoma Book, ISBN: 978-0-387-76699-7, Springer, Berlin
13. Poshtyar J, Shanbehzadeh, Ahmadieh H (2010) Automatic measurement of cup to disc ratio for diagnosis of glaucoma on retinal fundus images. Med Biometrics, 64–72
14. Vlachokosta PA, Asvestas GK, Matsopoulos N, Uzunoglu, Zeyen TG (2007) Preliminary study on the association of vessel diameter variation and glaucoma, in: Proceedings of 29th Annual International Conference on IEEE Engineering in Medicine and Biology Society, Lyon, pp 888–891
15. Wang Y, Yuan Y, Lei Z (2020) Fast SIFT feature matching algorithm based on geometric transformation. IEEE Access 8:88133–88140
16. Kun Z, Xiao M, Xinguo L (2019) Shape matching based on multi-scale invariant features. IEEE Access 7:115637–115649
17. Weinreb RN, Aung T, Medeiros FA (2014) The pathophysiology and treatment of glaucoma: A review. JAMA 311(18):1901. https://doi.org/10.1001/jama.2014.3192
18. Esteva A, Kuprel B, Novoa RA, Ko J, Swetter SM, Blau HM, Thrun S (2017) Dermatologist-level classification of skin cancer with deep neural networks. Nature 542(7639):115–118
19. Harmon SA, Sanford TH, Xu S, Turkbey EB, Roth H, Xu Z, Yang D, Myronenko A, Anderson V, Amalou A, Blain M (2020) Artificial intelligence for the detection of COVID-19 pneumonia on chest CT using multinational datasets. Nat Commun 11(1):4080
20. Gulshan V, Peng L, Coram M, Stumpe MC, Wu D, Narayanaswamy A, Venugopalan S, Widner K, Madams T, Cuadros J, Kim R (2016) Development and validation of a deep learning algorithm for detection of diabetic retinopathy in retinal fundus photographs. JAMA 316(22):2402–2410
21. Burlina PM, Joshi N, Pacheco KD, Freund DE, Kong J, Bressler NM (2018) Use of deep learning for detailed severity characterization and estimation of 5-year risk among patients with age-related macular degeneration. JAMA Ophthalmol 136(12):1359–1366
22. Dong Y, Zhang Q, Qiao Z, Yang J-J (2017) Classification of cataract fundus image based on deep learning. In: IEEE International Conference on Imaging Systems and Techniques (IST); 2017:1–5. https://doi.org/10.1109/IST.2017.8261463
23. Tan NYQ, Friedman DS, Stalmans I, Ahmed IIK, Sng CCA (2020) Glaucoma screening: where are we and where do we need to go? Curr Opin Ophthalmol 31(2):91–100. https://doi.org/10.1097/ICU.0000000000000649
24. Hemelings R, Elen B, Barbosa-Breda J, Lemmens S, Meire M, Pourjavan S, Vandewalle E, Van de Veire S, Blaschko MB, De Boever P, Stalmans I (2020) Accurate prediction of glaucoma from colour fundus images with a convolutional neural network that relies on active and transfer learning. Acta Ophthalmol 98(1):e94–e100
25. Thompson AC, Jammal AA, Medeiros FA (2019) A deep learning algorithm to quantify neuroretinal rim loss from optic disc photographs. Am J Ophthalmol 201:9–18. https://doi.org/10.1016/j.ajo.01.011
26. Sophia SSSJ, Diwakaran S (2023) Hybrid muddy electric fish and grasshopper optimization algorithm (MEF-GOA) based CNN for detection and severity differentiation of glaucoma in retinal fundus image. J Intell Fuzzy Syst, (Preprint), pp.1–19
27. Marino L (2017) Thinking chickens: a review of cognition, emotion, and behavior in the domestic chicken. Anim Cogn 20(2):127–147

28. Meng X, Liu Y, Gao X, Zhang H (2014) A new bio-inspired algorithm: chicken swarm optimization. In: Advances in Swarm Intelligence: 5th International Conference, ICSI 2014, Hefei, China, October 17–20, 2014, Proceedings, Part I 5. Springer International Publishing, pp 86–94
29. Deb S, Gao XZ, Tammi K, Kalita K, Mahanta P (2020) Recent studies on chicken swarm optimization algorithm: a review (2014–2018). Artif Intell Rev 53:1737–1765